Mutual neutralization in low-energy H⁺+H⁻ collisions: A quantum *ab initio* study

Michael Stenrup*

Department of Theoretical Chemistry, School of Biotechnology, Royal Institute of Technology, SE-106 91 Stockholm, Sweden

Åsa Larson and Nils Elander

Department of Physics, Stockholm University, AlbaNova University Center, SE-106 91 Stockholm, Sweden

The mutual neutralization of H⁺ and H⁻ at low collision energies is studied by means of a molecular close-coupling approach. All degrees of freedom are treated at the full quantum level also taking into account the identity of the nuclei. The relevant $^1\Sigma_g^+$ and $^1\Sigma_u^+$ electronic states as well as the associated nonadiabatic radial couplings are calculated for internuclear distances between 0.5 and $50a_0$. Following a transformation into a strictly diabatic basis, these quantities enter into a set of coupled equations for the motion of the nuclei. Numerical solution of these equations allows the cross sections for neutralization into the H(1)+H(n), $n=1,2,3$ final states to be calculated. In the present paper, results are reported for the collision energy region $0.001-100$ eV, with special emphasis on the important energy region below 10 eV. The low temperature rate coefficient is obtained from a parametrization of the calculated cross section and is estimated to be valid over the range $10-10\,000$ K.

PACS number(s): 34.70.+e, 31.50.Df, 31.50.Gh

I. INTRODUCTION

The mutual neutralization of H⁺ and H⁻ is the prototype reaction for electron transfer between two oppositely charged ions. With only two protons and two electrons involved, it is the simplest ion-ion reaction possible. Here, calculations should be able to provide accurate results, which could serve as benchmarks in the development of new theoretical methods and models. Furthermore, the reactants have well defined quantum states and are relatively easy to prepare in the laboratory. A detailed comparison between experiment and theory should thus be possible and should provide a natural starting point to understanding more complicated ion-ion collision phenomena. However, the simplicity of this reaction is deceptive, a fact which has stimulated a large number of studies in the past. Nevertheless, surprisingly few of these have investigated the neutralization cross section for collision energies below a few eV, which plays an important role in determining the H⁻ abundance in low temperature ionized environments. A compelling example from astrophysics is its influence on the gas phase formation of H_2, in particular, in the chemistry of the primordial gas, where one of the main reaction paths involves H⁻ as an intermediate [1–3].

Bates and Lewis [4] were the first to study the mutual neutralization of H⁺ and H⁻, which is written schematically as

$$H^+ + H^- \rightarrow H(1) + H(n),$$
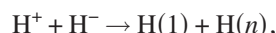
where n is the main quantum number of the excited hydrogen atom. Their calculations were based on the semiclassical Landau-Zener model [5,6] in which the reaction is thought to proceed along a system of horizontal covalent potential energy curves crossed by an attractive ion-pair potential. This pioneering study was later followed by others, among them

Olson *et al.* [7] and more recently, Eerden *et al.* [8]. Fussen and Kubach [9] have gone beyond the Landau-Zener concept and investigated the reaction at low collision energies using a one electron close-coupling model.

The only measurement of the neutralization cross section for collision energies below 3 eV is the merged beam experiment of Moseley *et al.* [10]. Their results seem to indicate a cross section that is approximately a factor of 3 higher than obtained in most of the cited theoretical studies. However, the theoretical results are mutually consistent and, for higher energies, also in more or less good agreement with the measurements reported by Szucs *et al.* [11] and Peart and Hayton [12]. This intriguing situation has led to the suspicion that the low energy cross section of Moseley *et al.* is overestimated [11–14].

In this paper we report results of a fully quantum mechanical *ab initio* study of the reaction at hand. We are mainly concerned with the collision energy region $0.001-10$ eV, but the calculations have been extended up to 100 eV in order to facilitate comparison with the cited experiments. The present study is based on a molecular close-coupling expansion of the total wave function. Accurate electronic structure methods have been used to calculate adiabatic states and nonadiabatic couplings of both gerade and ungerade symmetry over a wide range of internuclear distances. Subsequently, a transformation into a strictly diabatic representation has been performed and the diabatic quantities entered into a set of coupled equations for the motion of the nuclei. By numerically solving these equations, we have been able to calculate the neutralization cross sections for scattering within both the gerade and ungerade inversion symmetries. Finally, the identity of the nuclei has been accounted for by properly combining the gerade and ungerade cross sections.

The paper is organized as follows. Section II describes the theoretical framework underlying the present study. Section III describes the electronic structure calculations and discusses the resulting potential energy curves and coupling ma-

*stenrup@physto.se

trix elements. Section IV gives a brief account of the numerical treatment of the scattering problem. Section V presents and discusses the calculated neutralization cross sections and the reaction rate coefficient. Section VI concludes the paper and summarizes the main results. Unless stated otherwise, vector and matrix quantities are written in boldface and atomic units are used.

II. THEORY

A. Molecular expansion: Adiabatic and diabatic formulations

Consider a diatomic system composed of two nuclei and N electrons. The masses and charges of the nuclei are denoted by M_i and Z_i, respectively. Let $\mathbf{R}=(R, \theta, \varphi)$ be the internuclear separation vector and $\mathbf{r}_i$ a vector pointing from the center of mass of the nuclei to the ith electron. All vectors are expressed with respect to a space fixed axis system. For convenience, the notation $\mathbf{r}=(\mathbf{r}_1, \mathbf{r}_2, \ldots, \mathbf{r}_N)$ will occasionally be used. In these coordinates, the center of mass motion of the total system can be separated out, and the Hamiltonian takes the form [15]

$$H = -\frac{1}{2\mu}\nabla_{\mathbf{R}}^2 + H^{\mathrm{el}}, \tag{1}$$

where μ is the reduced mass of the nuclei and H^{el} is the electronic Hamiltonian. Neglecting terms of the form $[2(M_1+M_2)]^{-1}\nabla_{\mathbf{r}_i}\cdot\nabla_{\mathbf{r}_j}$, it follows that

$$H^{\mathrm{el}} = -\frac{1}{2}\nabla_{\mathbf{r}}^2 + \frac{Z_1 Z_2}{R} + \sum_{i>j=1}^{N}\frac{1}{|\mathbf{r}_i - \mathbf{r}_j|}$$
$$-\sum_{i=1}^{N}\left(\frac{Z_1}{\left|\frac{\mu}{M_1}\mathbf{R} + \mathbf{r}_i\right|} + \frac{Z_2}{\left|\frac{\mu}{M_2}\mathbf{R} - \mathbf{r}_i\right|}\right). \tag{2}$$

The total wave function $\psi(\mathbf{R}, \mathbf{r})$ satisfies the time-independent Schrödinger equation

$$H\psi(\mathbf{R}, \mathbf{r}) = E\psi(\mathbf{R}, \mathbf{r}), \tag{3}$$

where E is the total energy in the center of mass system. We expand $\psi(\mathbf{R}, \mathbf{r})$ in terms of electronic and nuclear states, $\phi_i^{\mathrm{a}}(\mathbf{R}, \mathbf{r})$ and $\chi_i^{\mathrm{a}}(\mathbf{R})$, according to

$$\psi(\mathbf{R}, \mathbf{r}) = \sum_{i=1}^{\infty} \phi_i^{\mathrm{a}}(\mathbf{R}, \mathbf{r})\chi_i^{\mathrm{a}}(\mathbf{R}) = \boldsymbol{\phi}^{\mathrm{a}}\boldsymbol{\chi}^{\mathrm{a}}, \tag{4}$$

where $\phi_i^{\mathrm{a}}(\mathbf{R}, \mathbf{r})$ are normalized solutions to the electronic Schrödinger equation

$$H^{\mathrm{el}}\phi_i^{\mathrm{a}}(\mathbf{R}, \mathbf{r}) = \epsilon_i^{\mathrm{a}}(R)\phi_i^{\mathrm{a}}(\mathbf{R}, \mathbf{r}). \tag{5}$$

The electronic energies $\epsilon_i^{\mathrm{a}}(R)$ depend parametrically on R and obey the noncrossing rule [16]. The particular choice of basis functions defined by Eq. (5) is called the adiabatic representation and is denoted by the superscript "a." Inserting the expansion (4) into Eq. (3) and using the orthonormality of the electronic states yields a set of coupled differential equations for the motion of the nuclei:

$$\left(-\frac{1}{2\mu}\mathbf{1}\nabla_{\mathbf{R}}^2 - \frac{1}{\mu}\mathbf{F}^{\mathrm{a}}\cdot\nabla_{\mathbf{R}} - \frac{1}{2\mu}\mathbf{G}^{\mathrm{a}} + \mathbf{V}^{\mathrm{a}}\right)\boldsymbol{\chi}^{\mathrm{a}} = E\mathbf{1}\boldsymbol{\chi}^{\mathrm{a}}, \tag{6}$$

with

$$\mathbf{F}_{ij}^{\mathrm{a}}(\mathbf{R}) = \langle\phi_i^{\mathrm{a}}|\nabla_{\mathbf{R}}|\phi_j^{\mathrm{a}}\rangle, \tag{7}$$

$$G_{ij}^{\mathrm{a}}(\mathbf{R}) = \langle\phi_i^{\mathrm{a}}|\nabla_{\mathbf{R}}^2|\phi_j^{\mathrm{a}}\rangle, \tag{8}$$

$$V_{ij}^{\mathrm{a}}(R) = \langle\phi_i^{\mathrm{a}}|H^{\mathrm{el}}|\phi_j^{\mathrm{a}}\rangle. \tag{9}$$

By definition, the matrix $\mathbf{V}^{\mathrm{a}}$ is diagonal and contains the adiabatic potential energy curves $\epsilon_i^{\mathrm{a}}(R)$. The matrix vector $\mathbf{F}^{\mathrm{a}}$ and the matrix $\mathbf{G}^{\mathrm{a}}$ both have off-diagonal elements, which are the nonadiabatic couplings between different electronic states. In addition, $\mathbf{G}^{\mathrm{a}}$ also has diagonal elements commonly referred to as adiabatic energy corrections. If the electronic wave functions are taken to be real, the chain rule for derivatives can be used to show that $\mathbf{F}^{\mathrm{a}}$ is antisymmetric, i.e.,

$$\mathbf{F}_{ij}^{\mathrm{a}}(\mathbf{R}) = -\mathbf{F}_{ji}^{\mathrm{a}}(\mathbf{R}). \tag{10}$$

The electronic states approximately correlate with the separated atomic limits and therefore each term in Eq. (4) defines a scattering channel. To determine the outcome of any collision process, we need to solve the coupled equations out to the asymptotic region where these limits are reached. However, it has been known for a long time that a product of the form $\chi_i^{\mathrm{a}}(\mathbf{R})\phi_i^{\mathrm{a}}(\mathbf{R}, \mathbf{r})$ does not properly describe the translational motion of the electrons along with the nuclei [17–19]. This can lead to difficulties of both formal and practical nature. One of the most prominent is the appearance of nonvanishing couplings at large or even infinite internuclear distances [18–20]. However, it is demonstrated in Sec. V B that the influence of these couplings on the present results is expected to be small.

The nonadiabatic coupling terms in Eq. (6) often vary rapidly with R and may cause problems in the numerical solution procedure. Furthermore, the presence of $\mathbf{F}^{\mathrm{a}}$ leads to differential equations that contain both first and second order derivatives. It is therefore desirable to transform Eq. (6) into an electronic basis where some or all of the nonadiabatic couplings disappear. Following Mead and Truhlar [21], we shall refer to a representation in which all three components of $\mathbf{F}^{\mathrm{a}}$ vanish as strictly diabatic. From this point on, it is assumed that the total wave function can be represented in a finite set of M adiabatic basis functions. The transformation may then be written in terms of an orthogonal matrix $T_{ij}(\mathbf{R})$ [22] as

$$\phi_i^{\mathrm{d}}(\mathbf{R}, \mathbf{r}) = \sum_{j=1}^{M} \phi_j^{\mathrm{a}}(\mathbf{R}, \mathbf{r})T_{ij}^{\mathrm{T}}(\mathbf{R}). \tag{11}$$

In order for the total wave function to be preserved, the nuclear states must transform according to

$$\chi_i^{\mathrm{d}}(\mathbf{R}) = \sum_{j=1}^{M} \chi_j^{\mathrm{a}}(\mathbf{R})T_{ij}^{\mathrm{T}}(\mathbf{R}). \tag{12}$$

Using the relation (12) to replace the adiabatic states in Eq. (6) yields after some manipulation,

$$\left(-\frac{1}{2\mu}\mathbf{1}\nabla_\mathbf{R}^2 - \frac{1}{\mu}\mathbf{F}^\mathrm{d}\cdot\nabla_\mathbf{R} - \frac{1}{2\mu}\mathbf{G}^\mathrm{d} + \mathbf{V}^\mathrm{d}\right)\chi^\mathrm{d} = E\mathbf{1}\chi^\mathrm{d}, \quad (13)$$

with

$$\mathbf{F}^\mathrm{d} = \mathbf{T}^\mathrm{T}(\mathbf{1}\nabla_\mathbf{R} + \mathbf{F}^\mathrm{a})\mathbf{T}, \quad (14)$$

$$\mathbf{G}^\mathrm{d} = \mathbf{T}^\mathrm{T}(\mathbf{1}\nabla_\mathbf{R}^2 + 2\mathbf{F}^\mathrm{a}\cdot\nabla_\mathbf{R} + \mathbf{G}^\mathrm{a})\mathbf{T}, \quad (15)$$

$$\mathbf{V}^\mathrm{d} = \mathbf{T}^\mathrm{T}\mathbf{V}^\mathrm{a}\mathbf{T}. \quad (16)$$

The first derivative coupling $\mathbf{F}^\mathrm{d}$ expressed in the new basis is seen to vanish provided that $\mathbf{T}$ is a solution to the equation

$$(\mathbf{1}\nabla_\mathbf{R} + \mathbf{F}^\mathrm{a})\mathbf{T} = \mathbf{0}. \quad (17)$$

In the special case where all electronic states have the same angular momenta projection onto the molecular axis, only the radial component of $\mathbf{F}^\mathrm{a}$ can be nonzero [21]. Equation (17) then reduces to

$$\left[\mathbf{1}\frac{d}{dR} + \boldsymbol{\tau}(R)\right]\mathbf{T}(R) = \mathbf{0}, \quad (18)$$

where

$$\tau_{ij}(R) = \left\langle\phi_i^\mathrm{a}\left|\frac{\partial}{\partial R}\right|\phi_j^\mathrm{a}\right\rangle. \quad (19)$$

Assuming that the first derivative couplings between the adiabatic states with $i\leq M$ and those with $i>M$ are zero; also $\mathbf{G}^\mathrm{d}$ can be shown to vanish [22]. The coupled equations then take the form

$$\left(-\frac{1}{2\mu}\mathbf{1}\nabla_\mathbf{R}^2 + \mathbf{V}^\mathrm{d}\right)\chi^\mathrm{d} = E\mathbf{1}\chi^\mathrm{d}. \quad (20)$$

In the strictly diabatic representation, the nonadiabatic couplings transform into off-diagonal elements of the potential matrix $\mathbf{V}^\mathrm{d}$ (electronic couplings) and as a consequence, the diagonal elements of this matrix (diabatic potentials) no longer obey the noncrossing rule. As will be illustrated in Sec. III C, the strictly diabatic representation may show little resemblance to the simple and intuitive curve crossing picture often referred to as diabatic.

B. Asymptotic boundary conditions and the integral cross section

The interpretation of $\chi_i^\mathrm{d}(\mathbf{R})$ is usually simplified by requiring that

$$\lim_{R\to\infty}\mathbf{T}(R) = \mathbf{1}, \quad (21)$$

which makes the adiabatic and the diabatic representations coincide in the region where the scattering wave function is evaluated. Thus, in any of the representations, the physical situation is that of an incoming plane wave in some entrance channel j, and outgoing spherical waves in all channels, which are energetically allowed. The direction of the incoming plane wave can be chosen along the space fixed z axis. If the potential falls off reasonably fast [23], the appropriate boundary conditions are given by

$$\chi_i^\mathrm{d}(\mathbf{R}) \underset{R\to\infty}{\sim} \delta_{ij}e^{ik_jz} + f_{ij}(E,\theta)\frac{e^{ik_iR}}{R}, \quad (22)$$

where $f_{ij}(E,\theta)$ is the scattering amplitude for entering the collision in channel j and leaving it in channel i. Since the potential matrix is spherically symmetric, the scattering amplitude is independent of the azimuthal angle φ. The asymptotic wave number k_i is defined as

$$k_i = [2\mu(E - E_i^\mathrm{th})]^{1/2}, \quad (23)$$

where $E_i^\mathrm{th} = \lim_{R\to\infty}V_{ii}^\mathrm{d}(R)$ is the corresponding threshold energy. In the case of a Coulomb potential, the exponents in Eq. (22) have to be modified with logarithmic phase factors, which arise due to the long-range nature of this interaction [23].

Evaluating the probability fluxes associated with the two terms in Eq. (22) leads to the familiar multichannel expression for the integral cross section:

$$\sigma_{ij}(E) = \frac{2\pi k_i}{k_j}\int_0^\pi |f_{ij}(E,\theta)|^2 \sin\theta d\theta. \quad (24)$$

If the adiabatic states are connected by nonvanishing couplings at infinity, neither the boundary condition (21) nor the scattering formalism developed below will be appropriate. In this case, the couplings can be manually cut at some large but finite internuclear distance. This procedure is usually justified if the collision energy is low enough, but its validity should be considered from case to case.

C. Scattering formalism

The conventional approach to solving Eq. (20) is to express $\chi^\mathrm{d}(\mathbf{R})$ in terms of a partial wave expansion,

$$\chi_i^\mathrm{d}(\mathbf{R}) = \frac{1}{R}\sum_{l=0}^\infty A_l u_{i,l}(R)P_l(\cos\theta), \quad (25)$$

where $P_l(\cos\theta)$ are the well known Legendre polynomials [24] and A_l are constants to be chosen so that the boundary conditions (22) are fulfilled. The radial wave functions $u_{i,l}(R)$ can be shown to satisfy the equations

$$\left[-\frac{1}{2\mu}\frac{d^2}{dR^2} + \frac{l(l+1)}{2\mu R^2}\right]u_{i,l}(R) + \sum_{j=1}^M V_{ij}^\mathrm{d}u_{j,l}(R) = Eu_{i,l}(R), \quad (26)$$

subject to the physical boundary conditions $u_{i,l}(0)=0$. If the corresponding derivatives $u'_{i,l}(0)$ are chosen appropriately, these equations have M linearly independent solutions, which can be combined into a square matrix $\tilde{\mathbf{u}}$. It follows that

$$\left(\mathbf{1}\frac{d^2}{dR^2} + \mathbf{Q}_l\right)\tilde{\mathbf{u}}_l = \mathbf{0}, \quad (27)$$

where

$$\mathbf{Q}_l = 2\mu(E\mathbf{1} - \mathbf{V}^\mathrm{d}) - \frac{l(l+1)}{R^2}\mathbf{1}. \quad (28)$$

It is now assumed that the potential matrix is diagonal beyond some radius ρ and here has elements corresponding to either pure Coulomb or pure short-range interactions. In this region, Eq. (27) is analytically solvable and the radial wave functions may be expressed in terms of the incoming and outgoing wave solutions, $\alpha_{ij,l}(R)$ and $\beta_{ij,l}(R)$, as defined in the Appendix. These are essentially the same as adopted by Johnson [25] but have been extended to cover the Coulomb case. Thus,

$$\widetilde{\mathbf{u}}_l(R) \underset{R \geqslant \rho}{=} \boldsymbol{\alpha}_l(R) - \boldsymbol{\beta}_l(R)\mathbf{S}_l, \qquad (29)$$

which defines the scattering matrix $\mathbf{S}_l$. Inserting this expression into the partial wave expansion (25) and comparing with the boundary conditions (22) leads to the well known formula

$$f_{ij}(E,\theta) = \frac{1}{2i(k_i k_j)^{1/2}} \sum_{l=0}^{\infty} (2l+1)(S_{ij,l}^{\text{oo}} - \delta_{ij})P_l(\cos\theta), \tag{30}$$

for the scattering amplitude in terms of the open-open or physical partition of $\mathbf{S}_l$. The integral cross section for scattering from channel j to channel i is readily evaluated to be

$$\sigma_{ij}(E) = \sum_{l=0}^{\infty} \sigma_{ij,l}(E), \qquad (31)$$

where

$$\sigma_{ij,l}(E) = \frac{\pi}{k_j^2}(2l+1)|S_{ij,l}^{\text{oo}} - \delta_{ij}|^2. \qquad (32)$$

Instead of working with $\mathbf{S}_l$ directly, it is convenient to introduce the reactance matrix $\mathbf{K}_l$ [26], which is defined by

$$\widetilde{\mathbf{u}}_l(R) \underset{R \geqslant \rho}{=} \mathbf{a}_l(R) - \mathbf{b}_l(R)\mathbf{K}_l, \qquad (33)$$

where $a_{ij,l}(R)$ and $b_{ij,l}(R)$ are regular and irregular solutions to Eq. (27) explicitly given in the Appendix. Combining the definitions above together with those from the Appendix leads to the relationship [25]

$$\mathbf{S}_l^{\text{oo}} = (1 + i\mathbf{K}_l^{\text{oo}})^{-1}(1 - i\mathbf{K}_l^{\text{oo}}), \qquad (34)$$

between the open-open partitions of $\mathbf{S}_l$ and $\mathbf{K}_l$. This expression resembles the Cayley transform and, since $\mathbf{S}_l^{\text{oo}}$ is both symmetric and unitary, implies that $\mathbf{K}_l^{\text{oo}}$ is real [23].

Finally, we introduce the logarithmic derivative

$$\mathbf{y}_l = \widetilde{\mathbf{u}}_l' \widetilde{\mathbf{u}}_l^{-1}, \qquad (35)$$

which transforms the radial Schrödinger equation into the numerically more stable matrix Riccati equation [27,28]

$$\mathbf{y}_l' + \mathbf{Q}_l + \mathbf{y}_l^2 = \mathbf{0}, \qquad (36)$$

while the boundary condition at the origin becomes that of a diagonal matrix with infinite elements. This is the set of coupled equations that we ultimately have to solve. The relationship between $\mathbf{y}_l$ and $\mathbf{K}_l$ is easily seen to be

$$\mathbf{K}_l = [\mathbf{y}_l(\rho)\mathbf{b}_l(\rho) - \mathbf{b}_l'(\rho)]^{-1}[\mathbf{y}_l(\rho)\mathbf{a}_l(\rho) - \mathbf{a}_l'(\rho)]. \quad (37)$$

D. Modifications in the case of identical nuclei

Up to this point in the discussion complications that might arise if the nuclei are identical have been ignored. These may be considered in two steps. Firstly, since the charges of the nuclei that enter H^{el} are equal, the electronic states will be either symmetric (gerade) or antisymmetric (ungerade) under inversion of $\mathbf{r}$. If the nuclei are labeled A and B, and $\alpha, \beta, \gamma, \ldots$ represent groups of electrons in some definite quantum states, each asymptotic channel will be a linear combination of two configurations, say $A(\alpha) + B(\beta)$ and $A(\beta) + B(\alpha)$. Such linear combinations cannot describe the situation where a nucleus is known to carry a certain number of electrons in a certain quantum state (unless $\alpha = \beta$). Localization of the electron cloud can be achieved by forming proper linear combinations of the gerade and ungerade solutions. The g/u symmetry is explicitly indicated as a superscript and the channel index i is allowed to include all other quantum numbers. The appropriate scattering amplitudes are then given by [23]

$$f_{ij}^{\text{di}}(E,\theta) = \frac{1}{2}[f_{ij}^g(E,\theta) + f_{ij}^u(E,\theta)], \qquad (38)$$

and

$$f_{ij}^{\text{ex}}(E,\theta) = \frac{1}{2}[f_{ij}^g(E,\theta) - f_{ij}^u(E,\theta)], \qquad (39)$$

corresponding to the direct and exchange reactions

$$A(\alpha) + B(\beta) \rightarrow A(\gamma) + B(\delta), \qquad (40)$$

and

$$A(\alpha) + B(\beta) \rightarrow A(\delta) + B(\gamma). \qquad (41)$$

Here, the amplitudes f_{ij}^g and f_{ij}^u are given by the usual formula (30) applied to the gerade and ungerade manifolds separately.

A second complication arises from the fact that the masses of the nuclei are also equal. Consequently, it is impossible to distinguish direct scattering in the direction θ from exchange scattering in the direction $\pi - \theta$. This effect can be accounted for by adding the direct and exchange amplitudes coherently. The fully symmetrized scattering amplitudes are [29]

$$f_{ij}^{\pm}(E,\theta) = f_{ij}^{\text{di}}(E,\theta) \pm f_{ij}^{\text{ex}}(E,\pi-\theta), \qquad (42)$$

where the sign depends on whether the spatial part of the wave function should be symmetric $(+)$ or antisymmetric $(-)$ under exchange of the nuclei. To illustrate this point we consider a hydrogen quasimolecule where the two protons are known to be in a singlet spin state. According to the Pauli principle, the total wave function (spin part included) must be antisymmetric under exchange of the nuclei. Since the singlet spin state itself is antisymmetric under such an operation, the spatial part of the wave function is forced to be symmetric. Thus, f_{ij}^+ is the appropriate choice of amplitude.

The integral cross section is obtained by taking the modulus square of Eq. (42) and integrating the result over the unit sphere:

$$\sigma_{ij}^{+}(E) = \sum_{l \text{ even}} \sigma_{ij,l}^{g}(E) + \sum_{l \text{ odd}} \sigma_{ij,l}^{u}(E), \qquad (43)$$

and

$$\sigma_{ij}^{-}(E) = \sum_{l \text{ odd}} \sigma_{ij,l}^{g}(E) + \sum_{l \text{ even}} \sigma_{ij,l}^{u}(E), \qquad (44)$$

where $\sigma_{ij,l}^{g}$ and $\sigma_{ij,l}^{u}$ are given by Eq. (32) applied to the gerade and ungerade manifolds, separately. The subscript even (odd) indicates that only even (odd) partial waves should be summed over. In the particular case of the hydrogen quasimolecule, the total spin state of the nuclei is either a singlet (para hydrogen) or a triplet (ortho hydrogen). Taking into account the degeneracy factors (1 and 3) and the exchange symmetry of these spin states, the symmetrized integral cross section for an ensemble of particles with randomly oriented spins is

$$\sigma_{ij}^{\text{sym}}(E) = \frac{1}{4} \sum_{l \text{ even}} \sigma_{ij,l}^{g}(E) + \frac{3}{4} \sum_{l \text{ odd}} \sigma_{ij,l}^{g}(E) + \frac{3}{4} \sum_{l \text{ even}} \sigma_{ij,l}^{u}(E)$$
$$+ \frac{1}{4} \sum_{l \text{ odd}} \sigma_{ij,l}^{u}(E). \qquad (45)$$

This can be compared with the expression

$$\sigma_{ij}^{\text{dist}}(E) = \frac{1}{2} \sum_{l=0}^{\infty} \sigma_{ij,l}^{g}(E) + \frac{1}{2} \sum_{l=0}^{\infty} \sigma_{ij,l}^{u}(E), \qquad (46)$$

obtained by treating the nuclei as distinguishable, and thus adding the direct and exchange amplitudes incoherently.

In deriving Eqs. (45) and (46) we have assumed that all final states exist in both gerade and ungerade versions. This is not always the case. Of particular interest to the present study are processes in which the final electronic state corresponds to $\gamma = \delta$ and exists only in a gerade version. In this case, Eqs. (45) and (46) are still valid (setting $\sigma_{ij,l}^{u} = 0$), although the arguments leading to these formulas are somewhat modified.

III. ELECTRONIC STRUCTURE CALCULATIONS

The electronic states relevant to the present study are those of H_2. The amount of data published for this system is of course substantial. Of particular relevance here are the very accurate electronic structure calculations reported by Wolniewicz and co-workers [30–36] using explicitly correlated basis functions and the calculations by Detmer *et al.* [37] using a nonspherical Gaussian basis set. Reactions like the present one, however, require the calculation of not only a large number of excited states but also the associated nonadiabatic couplings for a wide range of internuclear distances. To the best of our knowledge, a complete and accurate set of data for these quantities does not exist in the literature. We have therefore performed *ab initio* electronic structure calculations of all the relevant potential energy curves and nonadiabatic couplings. Where such data is available, our results have been compared with the benchmark calculations of Refs. [30–36].

TABLE I. Specification of the spherical Gaussian basis set used in the present study.

Type	Exponent	Type	Exponent
s[a]		p	0.0275700
s	0.7977000	p	0.0094220
s	0.2581000	p	0.0031910
s	0.0898900	p	0.0010470
s	0.0251300	d	2.0620000
s	0.0078770	d	0.6620000
s	0.0029256	d	0.1900000
s	0.0008852	d	0.0635300
s	0.0002917	d	0.0211100
p	2.2920000	d	0.0070570
p	0.8380000	d	0.0023460
p	0.2920000	f	1.3970000
p	0.0848000	f	0.3600000

[a]Contraction of six primitive s functions with exponents (82.64, 12.41, 2.824, 0.7977, 0.2581, 0.08989) and coefficients (0.002 006, 0.015 343, 0.075 579, 0.256 875, 0.497 368, 0.296 133).

A. Potential energy curves

We have calculated the adiabatic potential energy curves and the associated electronic wave functions corresponding to the seven lowest $^1\Sigma_g^+$ states and the six lowest $^1\Sigma_u^+$ states, here denoted as $(1-7)^1\Sigma_g^+$ and $(1-6)^1\Sigma_u^+$, respectively. All calculations have been performed at the full configuration interaction (FCI) level using a modified version of the DALTON 2.0 program package [38]. The molecular orbitals have been obtained in an $(11s, 8p, 7d, 2f)$ spherical Gaussian basis set contracted to $[9s, 8p, 7d, 2f]$. The compact basis functions of this set have been taken from the augmented correlation-consistent polarized valence quadruple zeta (aug-cc-pVQZ) basis set of Dunning and co-workers [39,40], while the more diffuse ones have been approximately optimized to obtain a good representation of the excited states. The basis set is given in Table I.

Figure 1 shows the $(2-7)^1\Sigma_g^+$ and $(1-6)^1\Sigma_u^+$ potential energy curves in the range $0.5-50a_0$. As is well known, only one bound state of the negative hydrogen ion exists, the $^1S^e$ ground state [41]. Accordingly, there is one gerade and one ungerade electronic state that asymptotically correlate with the $H^+ + H^-$ ion-pair limit. As the internuclear distance is decreased from infinity, the ion-pair configuration is successively carried on through a series of avoided crossings involving states correlated with the $H(1) + H(n)$ covalent limits. In the neighborhood of these crossings, the first derivative radial couplings (19) are significant and are able to cause transitions between different adiabatic states.

Beginning with the gerade symmetry, the $(1-6)^1\Sigma_g^+$ manifold consists of states correlated with the $n = 1, 2, 3$ covalent limits. Corresponding to each limit $H(1) + H(n)$ there are n of these states in total. The $7^1\Sigma_g^+$ state has the ion-pair configuration from $36a_0$ up to approximately $280a_0$. Here, the adiabatic wave function changes character into the $n = 4$ covalent configuration while the ion-pair configuration is carried on to
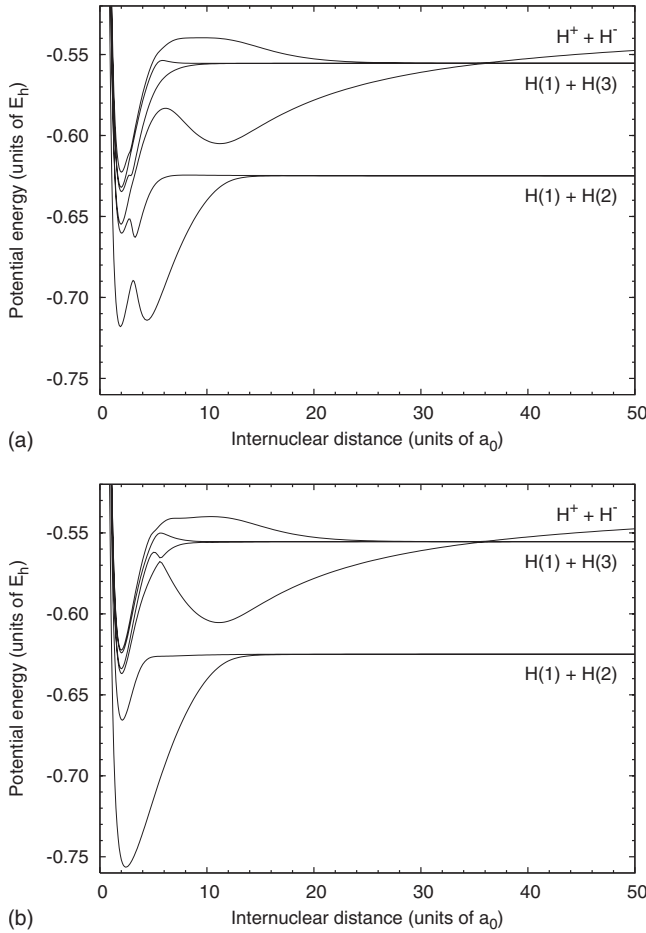
FIG. 1. Adiabatic potential energy curves for (a) the $(2-7)^1\Sigma_g^+$ states and (b) the $(1-6)^1\Sigma_u^+$ states of H_2. The separated atomic limits are indicated at the far right of each subfigure. For a discussion of the particular ion-pair limit, see the main text.

another higher excited state. At such large distances, however, the motion of the nuclei is highly diabatic and the change of character of the adiabatic wave functions will not induce any significant ionic-covalent transitions [4,42,43]. With these considerations in mind, we will refer to the $7^1\Sigma_g^+$ state as that which is correlated with the ion-pair limit.

In the ungerade symmetry, the $(1-5)^1\Sigma_u^+$ manifold consists of states correlated with the $n=2,3$ covalent limits while the $6^1\Sigma_u^+$ state, with the same considerations as above, can be said to correlate with the ion-pair limit. Because of symmetry restrictions, there can be no singlet ungerade state dissociating into the $n=1$ covalent limit. Note that while the gerade and ungerade states behave very differently at small internuclear distances, these differences vanish quickly as the separation of the nuclei is increased. In fact, at $10a_0$ the energy difference for all excited states is less than $9 \times 10^{-4}E_h$ (Hartree) and at $30a_0$ it is less than $5 \times 10^{-5}E_h$.

Figure 1 illustrates the two avoided crossings near 12 and $36a_0$, which are related to a change from ionic to $n=2$ and 3 covalent character (or vice versa) of the adiabatic wave functions. In what follows we will refer to them simply as the $n=2$ and 3 curve crossings. Figure 1 also shows a rich pattern of avoided crossings taking place at

smaller internuclear distances. This region, however, is to a large extent shielded by the centrifugal term in Eq. (26) and the influence of the resulting radial couplings upon the total neutralization cross section is rather small (see Sec. V B). The higher excited $^1\Sigma_{g,u}^+$ states that are not considered in the present study are only accessible to the system through avoided crossings at small internuclear distances [37]. The error introduced by excluding these states is therefore expected to be of less significance. In principle, also rotational couplings to states of $^1\Pi$ symmetry should be considered. However, due to the presence of strong radial couplings in the vicinity of the $n=2$ and 3 curve crossings, and due to the low collision energies considered in the present study, these are assumed to be negligible [9,44].

To evaluate the quality of our calculated potential energy curves, we have compared them with those reported by Wolniewicz and co-workers. Their calculations cover the $1^1\Sigma_g^+$ state out to $12a_0$ [32,34], the $(2-6)^1\Sigma_g^+$ states out to $20a_0$ [33], and the $(1-6)^1\Sigma_u^+$ states out to $150a_0$ [36]. The potential energy curve for the $4^1\Sigma_g^+$ state has been recalculated and extended out to $80a_0$ [35]. With the energy scale used in Fig. 1, these potentials would entirely overlap with ours. A more detailed comparison shows that the largest energy difference is obtained for the inner part ($R \lesssim 1.5a_0$) of the $1^1\Sigma_g^+$ ground state potential, which is of little importance to the present study anyway. Here, our computed values are approximately 5.7×10^{-4} to $1.5 \times 10^{-3}E_h$ higher in energy compared to those in Ref. [34]. For all of the excited states, our calculated energies are approximately 1.0×10^{-4} to $5.6 \times 10^{-4}E_h$ higher than in Refs. [33,35,36]. It is of particular interest to estimate the quality of the $(4-7)^1\Sigma_g^+$ and $(3-6)^1\Sigma_u^+$ states near the critical $n=3$ curve crossing. Concerning the ungerade states, the covalent parts of our potentials are within $1.6 \times 10^{-4}E_h$ and the ionic parts within $3.0 \times 10^{-4}E_h$ to those reported in Ref. [36]. Due to the near degeneracy of the gerade and ungerade states, we expect this accuracy to be common to both inversion symmetries. The quality of the adiabatic states and, in particular, their energy splitting at the $n=3$ curve crossing will be discussed further in the next section.

B. Radial couplings

We have calculated the first derivative radial couplings (19) between all of the adiabatic states considered in the previous section. The accurate evaluation of these quantities is not trivial. The magnitude and shape of the radial couplings are usually very sensitive to the quality of the electronic wave functions and it is essential that not only the individual states are good in a variational sense, but also that the relative energies of these states are well represented. In regions where two or more adiabatic states become nearly degenerate, further complexity is added by the fact that a minor change in the atomic basis can cause the potential energy curves to artificially pseudocross, giving rise to dramatic effects in the radial couplings. These effects do not change the outcome of the dynamics but can obscure both interpretation and comparison with other results.

To evaluate the radial couplings we have implemented a three point version of the finite difference method described

in Ref. [45]. This method provides a systematic way to converge the calculations toward the exact result in the particular type of basis and wave function being considered. We have examined carefully how the calculated radial couplings depend on the derivative step length ΔR, as well as the numerical accuracies δ_{MO} and δ_{CI}, with which the molecular orbitals and the CI wave functions are obtained. Stable and converged results were observed when $\Delta R = 5 \times 10^{-5} a_0$, $\delta_{MO} = 10^{-14} E_h$, and $\delta_{CI} = 10^{-13} E_h$. The antisymmetry condition (10) can be used as a simple consistency check of the results. In the present case, most of the calculated coupling elements satisfied this condition to at least four significant digits. For practical reasons, it is still desirable to have a coupling matrix that is fully antisymmetric. This has been accomplished by taking each element to be the geometrical mean of τ_{ij} and $-\tau_{ji}$.

The radial couplings are too many to discuss in full detail and so we will focus on those relevant for the important $n=2$ and 3 curve crossings. The notation $(i,j)_g$ is used to label the radial coupling between the ith and jth $^1\Sigma_g^+$ state (and similarly for the ungerade states). Due to symmetry,

FIG. 3. Radial couplings among the $(4-7)^1\Sigma_g^+$ states in the neighborhood of the $n=3$ curve crossing. The notation $(i,j)_g$ label the radial coupling between the ith and jth $^1\Sigma_g^+$ state.

gerade and ungerade states are not coupled to each other.

In Fig. 2 we show the radial couplings among the $(2-4)^1\Sigma_g^+$ and $(1-3)^1\Sigma_u^+$ states in the neighborhood of the $n=2$ curve crossing. As can be expected from the appearance of the potential energy curves, each of the $(2,4)_g$ and $(1,3)_u$ couplings show a rather broad peak near the crossing point at $12a_0$ resulting from the exchange of ionic and $n=2$ covalent character between the adiabatic wave functions. Similar shapes and magnitudes, although displaced to larger internuclear distances, are also exhibited by the $(2,3)_g$ and $(1,2)_u$ couplings, which connect the adiabatic states tending to the $n=2$ covalent limit. The $(3,4)_g$ and $(2,3)_u$ couplings are, on the other hand, much less pronounced in the crossing region. For comparison, also plotted in Fig. 2 are the results obtained by Wolniewicz and Dressler [30,33], which include the radial couplings among all of the $(2-4)^1\Sigma_g^+$ states and between the 1 and $2^1\Sigma_u^+$ states. The overall agreement with the present results is very good, in particular, in the region up to approximately $16a_0$. For larger internuclear distances some deviations can be observed. These are most likely due to a slight unbalance in our description of the nearly degenerate $n=2$ adiabatic states. However, as mentioned at the very beginning of this section, the physical relevance of these types of effects is expected to be small.

Figure 3 illustrates the radial couplings among the adiabatic states associated with the $n=3$ curve crossing. Here, the gerade and ungerade states are almost completely degenerate and so only the results for the former of these, i.e., the $(4-7)^1\Sigma_g^+$ manifold of states, are shown. All the couplings appear as peaklike structures with their maxima located in the region $35.5-37.0a_0$. The most prominent of these is the $(4,7)_g$ coupling, which reaches its maximum value at $35.9a_0$. This coupling arises from the exchange of ionic and $n=3$ covalent character between the 4 and $7^1\Sigma_g^+$ adiabatic states. We note that the location of its maximum agrees well with the crossing point of the pure ionic and covalent energies at $36.0a_0$ obtained from the ground state energy [46] and the polarizability [47] of the H⁻ ion. The calculations of Wolniewicz and Dressler do not extend out to the $n=3$ curve crossing and thus no direct comparison of the radial cou-
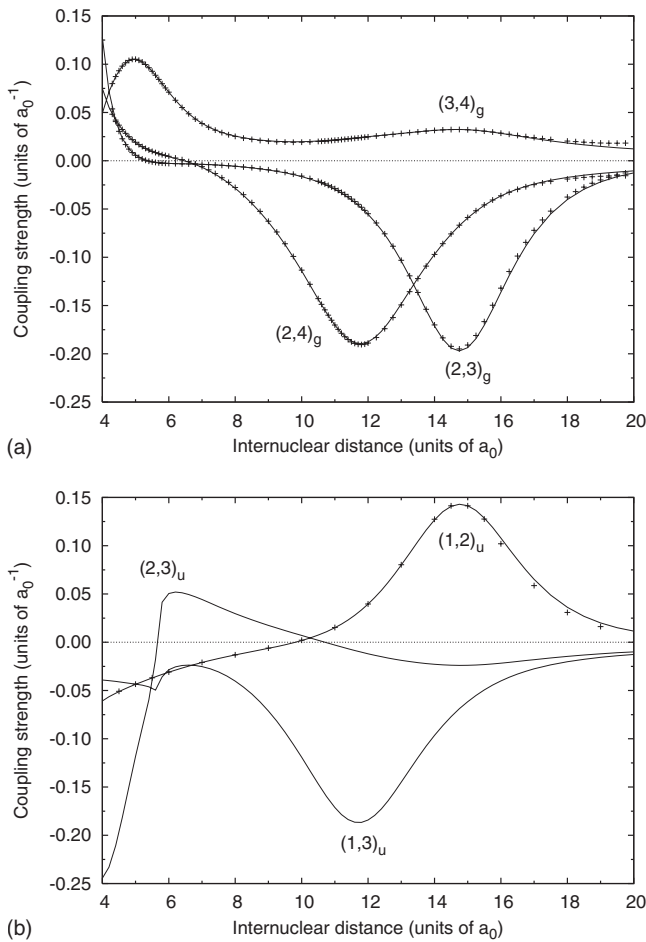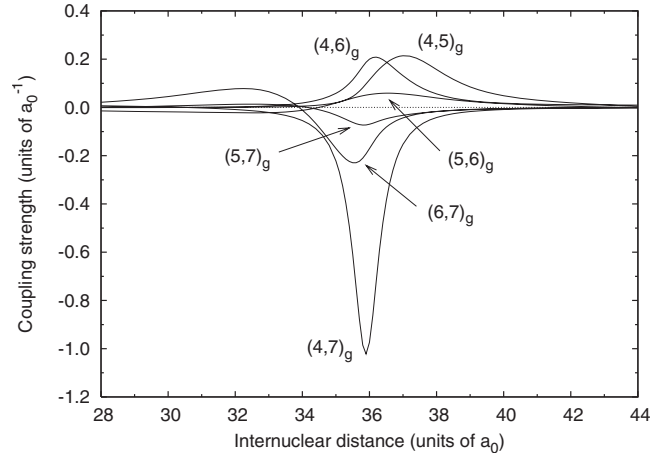

FIG. 2. Radial couplings among (a) the $(2-4)^1\Sigma_g^+$ states and (b) the $(1-3)^1\Sigma_u^+$ states in the neighborhood of the $n=2$ curve crossing. The notation $(i,j)_g$ labels the radial coupling between the ith and jth $^1\Sigma_g^+$ state (and similarly for the ungerade states). The present results (solid lines) are compared with the results obtained by Wolniewicz and Dressler (crosses) [30,33].
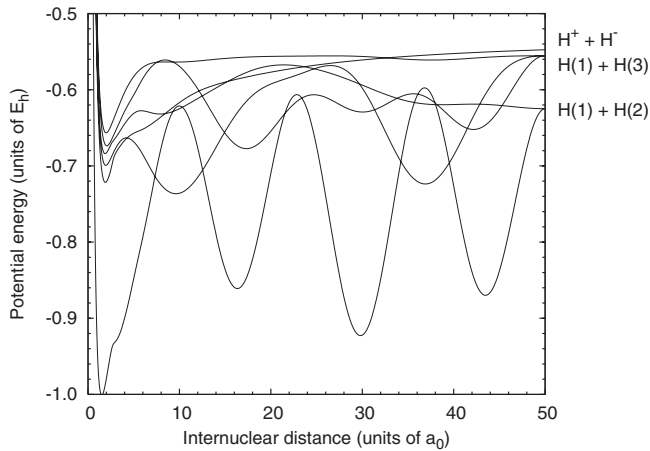
FIG. 4. Strictly diabatic potential energy curves obtained from a transformation of the $(1-7)^1\Sigma_g^+$ adiabatic states. The diabatic potential energy curve associated with the H(1)+H(1) limit is not shown in the figure.

plings can be made. However, in the ungerade symmetry we can compare the energy splitting of the 3 and $6^1\Sigma_u^+$ states at $35.9a_0$. Here, we obtain the value $3.8 \times 10^{-4}E_h$, which is in very good agreement with the value $3.9 \times 10^{-4}E_h$ calculated from the results of Ref. [36].

C. Adiabatic to diabatic transformation

In order to obtain the adiabatic to diabatic transformation (ATDT) matrix, we have numerically solved Eq. (18) using the radial couplings described in the preceding section as input data. The solution has been obtained with a matrix version of the Runge-Kutta Fehlberg method [48]. The boundary condition $\mathbf{T}=\mathbf{1}$ has been imposed at $R=50a_0$ and the integration has been performed inwards. As hinted above, several of the nonadiabatic couplings are nonvanishing as R tends to infinity. In practice, our choice of boundary condition corresponds to setting these couplings to zero beyond $50a_0$. Since this kind of assumption has to be made in the calculation of the scattering matrix anyway, no additional error is introduced due to the diabatization procedure itself. In the present case, the transformation to a strictly diabatic basis is merely for computational reasons and is not discussed further. It is worth noting, however, that the diabatic potential energy curves we obtain here are far from the intuitive ones conventionally used in connection with the H_2 system (see Fig. 4).

IV. NUMERICAL PROCEDURES

The logarithmic derivative (35) has been calculated by numerically solving the matrix Riccati equation (36) from $0.54a_0$ out to $50a_0$. For this purpose we have used an algorithm developed by Johnson [27,28] with the grid size set to $5 \times 10^{-3}a_0$. Knowledge of the logarithmic derivative in the final integration point has allowed us to calculate the partial cross sections (32) for scattering within the gerade and ungerade inversion symmetries. The fully symmetrized integral cross sections have been obtained by combining the partial
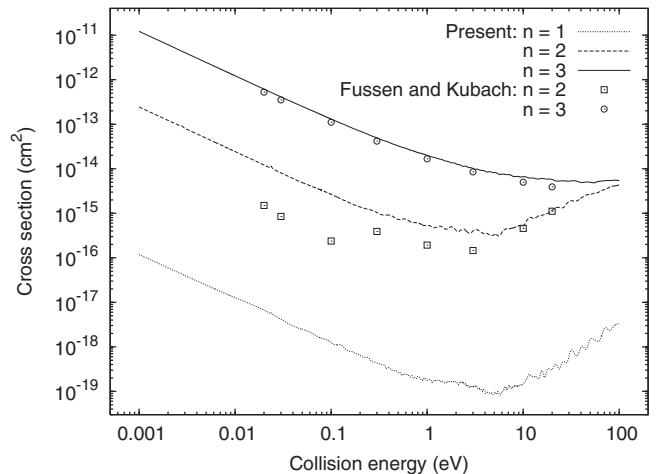

FIG. 5. Calculated cross sections for scattering into the H(1)+H(n), $n=1,2,3$ final states. The present results are compared with the close-coupling results of Fussen and Kubach [9].

cross sections according to Eq. (45). To determine at which point the series in Eq. (45) could be truncated, a simple convergence criteria was introduced. This was set to terminate the summation if the ratios of the partial cross sections and the accumulated integral cross sections remained less than 10^{-4} for 25 terms in succession. Over the energy range considered here, this led to the inclusion of approximately 250–3500 partial waves.

V. RESULTS AND DISCUSSION

A. State-dependent cross sections

The calculated cross sections for scattering into the H(1)+H(n), $n=1,2,3$ final states are shown in Fig. 5. It is clear that the $n=3$ process dominates the others over almost the entire energy range, which is reasonable considering the favorable location of the $n=3$ curve crossing at around $36a_0$. In contrast, the $n=2$ transitions occur much further in and are more easily suppressed by the centrifugal barrier. Only for collision energies above 5 eV, where the $n=2$ cross section exhibits a minimum, is this process able to compete with neutralization into the $n=3$ final states. This phenomena was first noted by Bates and Lewis [4] and has been confirmed, at least on a qualitative level, by almost every study since then [7–9]. Neutralization into the $n=1$ final state is insignificant at all energies and is included only for completeness. As the collision energy approaches zero, all cross sections gain the characteristic E^{-1} dependence that can be expected for reactions which are governed by the Coulomb interaction. Here, the $n=3$ cross section is approximately a factor of 50 larger than the $n=2$ cross section.

Some weaker oscillations can be observed over a large part of the energy range. The reason for this structure is not completely clear, but the most likely explanation is in terms of Stückelberg oscillations, i.e., in terms of quantum interference arising because there are several competing routes through the potential landscape leading to the same asymptotic limit.
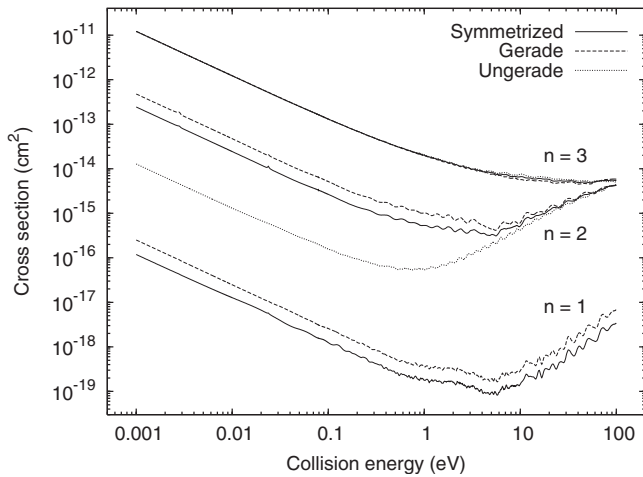
FIG. 6. Fully symmetrized vs pure gerade and ungerade cross sections for scattering into the $H(1)+H(n)$, $n=1,2,3$ final states.

The close-coupling results of Fussen and Kubach [9] have also been plotted in Fig. 5 for comparison. The agreement between their $n=3$ cross section and the present one is good. The difference is about 20 percent at 1 eV and increases slightly with the energy. Comparing the $n=2$ cross sections, the two calculations are seen to agree well above the minimum at 5 eV, whereas at lower energies the differences are more pronounced. A rationale for this discrepancy may be found by considering how the inversion symmetry of the electronic states is approached.

For this purpose we show in Fig. 6 a comparison of our fully symmetrized cross sections (same as in Fig. 5) together with the pure gerade and ungerade cross sections calculated in the conventional way. We first note that the $n=3$ cross section is fairly insensitive to the choice of inversion symmetry over the whole energy range. Consequently, the effect of averaging over these symmetries is expected to be small. A similar observation can be made regarding the $n=2$ cross section above 5 eV. However, at lower energies the gerade and ungerade results differ strongly. This indicates not only

that our way of combining the gerade and ungerade cross sections will affect the final result, but also that any two approaches that treat the inversion symmetry differently may lead to different outcomes. In the one electron model of Fussen and Kubach, this inversion symmetry is actually broken, and as a consequence their results are likely to differ from ours. It should be emphasized though, that at the energies where this happens the contribution from the $n=2$ channels to the overall reaction is small. It should also be noted that the effects of treating the nuclei as indistinguishable are very small, and it is equally good to use the simpler formula (46) in favor of Eq. (45) to weight the gerade and ungerade partial cross sections.

B. Total neutralization cross section

In Fig. 7 we show the calculated total neutralization cross section, i.e., the sum of the $n=1,2,3$ cross sections. As could be expected from the previous subsection, this cross section shows a rather smooth behavior over the entire energy range. At low collision energies, the curve approximately resembles the E^{-1} behavior discussed above. The cross section then continues to fall off until it reaches a broad minimum at around 20 eV. This minimum obviously results from the nearly constant $n=3$ cross section in combination with the rapid increase in the formation of $n=2$ final products.

To examine the influence of the nonvanishing asymptotic couplings upon the cross section, the point at which the logarithmic derivative is evaluated has been varied over the range $50-80a_0$. The boundary condition on the ATDT matrix has been varied accordingly. At the collision energies 0.001, 1, and 100 eV, the relative variation in the cross section was seen to be 4×10^{-4}, 7×10^{-4}, and 1×10^{-3}, respectively. We conclude that the effects of the nonvanishing asymptotic couplings over the energy range considered here are negligible. This is consistent with the conclusions drawn by Borondo *et al.* [43].

Additional tests have been performed in order to estimate the relevance of the radial couplings at small internuclear
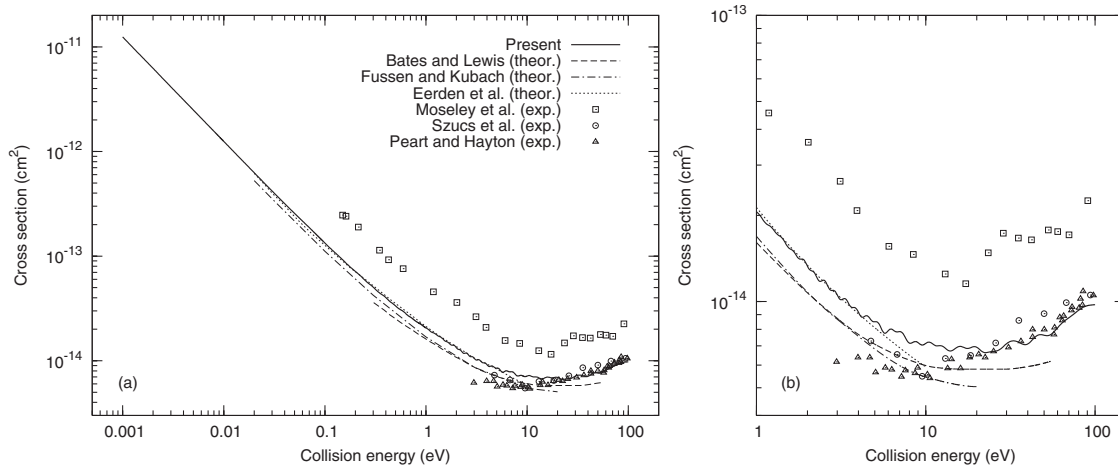

FIG. 7. Total cross section for the mutual neutralization of H⁺ and H⁻. The present results are compared with the measurements by Moseley *et al.* [10], Szucs *et al.* [11], and Peart and Hayton [12], as well as the calculations by Bates and Lewis [4], Fussen and Kubach [9], and Eerden *et al.* [8]. (a) Cross sections plotted over the full energy range $0.001-100$ eV. (b) Enlargement of the energy range $1-100$ eV.

distances (as discussed in Sec. III A). This has been done by setting all radial couplings up to a certain distance R_0 to zero before the diabatization procedure is carried out. Choosing $R_0 = 6a_0$ reduces the total neutralization cross section at 0.001, 1, and 100 eV collision energy by 8.6, 9.9, and 5.9 percent, respectively. These variations in the cross section can be considered small (although not insignificant) and may be taken as an upper limit for the influence of the higher lying $^1\Sigma_{g,u}^+$ adiabatic states not included in the present study, which are coupled to the lower lying states mainly at small internuclear distances. A more detailed study of these effects is currently being pursued.

In Fig. 7 we also show the results of earlier studies relevant for the mutual neutralization of H$^+$ and H$^-$ at low collision energies. Up to the present date, no measurements of this cross section have been reported for collision energies below 0.15 eV. In the region 0.15–3 eV, the only experimental results that are available are those of Moseley *et al.* [10]. A comparison shows that these are a factor of 2 to 3 larger than the present data. At energies above a few eV, experiments have been conducted by Szucs *et al.* [11] and Peart and Hayton [12], among others. In the region 3–10 eV, their results point towards a cross section that is slightly lower than ours, which is most evident for the first few data points of Peart and Hayton, whereas for collision energies above 10 eV all three studies agree favorably. Compared with earlier theoretical studies, our results match within 30% the close-coupling calculations of Fussen and Kubach [9] and within 40% the Landau-Zener calculations of Bates and Lewis [4]. Our results also more or less overlap with the Landau-Zener results obtained by Eerden *et al.* [8].

It may be worthwhile to review the accumulated data on the mutual neutralization of H$^+$ and H$^-$ at low collision energies (below a few eV). There are now several calculations of this cross section that are mutually consistent within a few tens of percent. These employ such diverse methods as semiclassical Landau-Zener theory as well as model Hamiltonian and *ab initio* close-coupling schemes. In the upper part of the energy region, the theoretical results are in more or less agreement with several of the available experiments. One of these might even suggest a cross section that is slightly lower than predicted by theory. It is a fact, however, that the only measurement that has been published for collision energies below 3 eV shows a cross section that is considerably higher than others reported. To clarify this situation, new experimental efforts are obviously required. Recently, such measurements have been undertaken by the group of Urbain [49] at the Université Catholique de Louvain, Belgium, using a merged beam apparatus in the energy range 0.001–0.2 eV. Although uncertainties of the order of 50% still exist, preliminary results from this experiment seem to support the neutralization cross section obtained from the various theoretical treatments.

C. Rate coefficient

At low collision energies, the total neutralization cross section may be parametrized in terms of the relative velocity v as [10]

$$\sigma(v) = Av^{-2} + Bv^{-1} + C + Dv. \qquad (47)$$

To determine the unknown coefficients of this expression, we have performed a least square fit to our calculated cross section in the region 0.001–4 eV. The result is

$$A = 4.77 \times 10^{-2} \text{ cm}^4 \text{ s}^{-2},$$

$$B = -1.73 \times 10^{-9} \text{ cm}^3 \text{ s}^{-1},$$

$$C = 1.22 \times 10^{-14} \text{ cm}^2,$$

$$D = -1.57 \times 10^{-21} \text{ cm s},$$

corresponding to a maximum error of 6% in the parametrized cross section. By integrating Eq. (47) over a Maxwellian velocity distribution, the associated rate coefficient $\alpha(T)$ is obtained as follows:

$$\alpha(T) = A\left(\frac{2\mu}{\pi kT}\right)^{1/2} + B + 2C\left(\frac{2kT}{\pi\mu}\right)^{1/2} + \frac{3DkT}{\mu}, \quad (48)$$

where T is the ion temperature and k is the Boltzmann constant. We estimate the above results to be valid over the temperature range 10–10 000 K. For comparison, the rate coefficient we obtain at 300 K is $1.73 \times 10^{-7} \text{cm}^3 \text{ s}^{-1}$.

VI. SUMMARY

In this paper we have considered the mutual neutralization of H$^+$+H$^-$ into H(1)+H(n), $n = 1, 2, 3$ at low collision energies. To arrive at the present results, we have used a molecular close-coupling approach with all degrees of freedom treated quantum mechanically. Adiabatic potential energy curves and nonadiabatic radial couplings have been calculated at the FCI level of theory employing a large Gaussian basis set. These quantities are in good agreement with those obtained from more sophisticated electronic structure methods [30–36]. Using a strictly diabatic representation of the potential energy curves and coupling matrix elements, we have calculated state-dependent and total neutralization cross sections taking into account the identity of the nuclei.

The present results conform to the conventional view that for collision energies up to a few eV, almost all neutral products go into the $n = 3$ final states. Furthermore, a proper weighting of the gerade and ungerade cross sections turns out to be important only for the $n = 2$ formation at low collision energies, where these cross sections anyway are small. In the collision energy region below a few eV, our total neutralization cross section is in good agreement with previous theoretical studies [4,8,9], but is a factor of 2 to 3 lower than that measured by Moseley *et al.* [10].

APPENDIX

Here, we provide analytical expressions for the solution matrices $\mathbf{a}_l$, $\mathbf{b}_l$, $\boldsymbol{\alpha}_l$, and $\boldsymbol{\beta}_l$, which are used in the definitions of the reactance and scattering matrices of Sec. II C. Open and closed channels are distinguished depending on whether the total energy is greater or less than the corresponding threshold energy. The channels are labeled short range (covalent) if

$$V_{ii}^{\mathrm{d}}(R) \underset{R \geqslant \rho}{=} E_i^{\mathrm{th}}, \tag{A1}$$

and Coulombic if

$$V_{ii}^{\mathrm{d}}(R) \underset{R \geqslant \rho}{=} E_i^{\mathrm{th}} + \frac{Q_1 Q_2}{R}, \tag{A2}$$

where Q_1 and Q_2 are the net charges situated on each of the nuclei. The asymptotic wave number k_i for open channels has been defined in Eq. (23). For closed channels,

$$k_i = [2\mu(E_i^{\mathrm{th}} - E)]^{1/2}. \tag{A3}$$

It is further convenient to introduce the scaled coordinate $\xi_i = k_i R$ and the Coulomb parameter

$$\eta_i = \frac{\mu Q_1 Q_2}{k_i}. \tag{A4}$$

We look for pairs of linearly independent solutions to the radial Schrödinger equation (27) in the region $R \geqslant \rho$. These are chosen such that $a_{ii,l}(R)$ and $b_{ii,l}(R)$ behave as regular and irregular solutions, and $\alpha_{ii,l}(R)$ and $\beta_{ii,l}(R)$ as incoming and outgoing wave solutions, respectively. For open short-range channels, two linearly independent solutions are the Riccati-Bessel functions of the first and second kind, $\widetilde{S}_l(\xi_i)$ and $\widetilde{C}_l(\xi_i)$, respectively [24]. We adopt the definitions [25]

$$a_{ij,l} = \delta_{ij} k_i^{-1/2} \widetilde{S}_l, \tag{A5}$$

$$b_{ij,l} = \delta_{ij} k_i^{-1/2} \widetilde{C}_l, \tag{A6}$$

$$\alpha_{ij,l} = \delta_{ij} k_i^{-1/2} (-i\widetilde{S}_l + \widetilde{C}_l), \tag{A7}$$

$$\beta_{ij,l} = \delta_{ij} k_i^{-1/2} (i\widetilde{S}_l + \widetilde{C}_l). \tag{A8}$$

For open Coulomb channels, the radial Schrödinger equation is solved by the regular and irregular Coulomb functions $\widetilde{F}_l(\eta_i, \xi_i)$ and $\widetilde{G}_l(\eta_i, \xi_i)$, respectively [24]. Accordingly,

$$a_{ij,l} = \delta_{ij} k_i^{-1/2} \widetilde{F}_l, \tag{A9}$$

$$b_{ij,l} = \delta_{ij} k_i^{-1/2} \widetilde{G}_l, \tag{A10}$$

$$\alpha_{ij,l} = \delta_{ij} k_i^{-1/2} (-i\widetilde{F}_l + \widetilde{G}_l), \tag{A11}$$

$$\beta_{ij,l} = \delta_{ij} k_i^{-1/2} (i\widetilde{F}_l + \widetilde{G}_l). \tag{A12}$$

Finally, in the case of closed short-range channels, possible solutions are $\xi_i \widetilde{i}_l(\xi_i)$ and $\xi_i \widetilde{k}_l(\xi_i)$, where $\widetilde{i}_l(\xi_i)$ and $\widetilde{k}_l(\xi_i)$ are the modified spherical Bessel functions of the first and second kind, respectively [24] (first and third kind in the cited reference). Appropriate definitions are [25]

$$a_{ij,l} = \delta_{ij} 2^{1/2} \pi^{-1/2} \xi_i \widetilde{i}_l, \tag{A13}$$

$$b_{ij,l} = \delta_{ij} 2^{1/2} \pi^{-1/2} \xi_i \widetilde{k}_l, \tag{A14}$$

$$\alpha_{ij,l} = \delta_{ij} (2\pi)^{1/2} \xi_i k_i^{-1} [\widetilde{i}_l + (-1)^l \pi^{-1} \widetilde{k}_l], \tag{A15}$$

$$\beta_{ij,l} = \delta_{ij} 2^{1/2} \pi^{-1/2} \xi_i k_i^{-1} \widetilde{k}_l. \tag{A16}$$

Closed Coulomb channels play no role in the present study and are therefore not considered.

[1] D. Galli and F. Palla, Astron. Astrophys. **335**, 403 (1998).
[2] S. C. O. Glover, Astrophys. J. **584**, 331 (2003).
[3] S. C. Glover, D. W. Savin, and A.-K. Jappsen, Astrophys. J. **640**, 553 (2006).
[4] D. R. Bates and J. T. Lewis, Proc. Phys. Soc., London, Sect. A **68**, 173 (1955).
[5] L. Landau, Phys. Z. Sowjetunion **2**, 46 (1932).
[6] C. Zener, Proc. R. Soc. London, Ser. A **137**, 696 (1932).
[7] R. E. Olson, J. R. Peterson, and J. Moseley, J. Chem. Phys. **53**, 3391 (1970).
[8] M. J. J. Eerden, M. C. M. van de Sanden, D. K. Otorbaev, and D. C. Schram, Phys. Rev. A **51**, 3362 (1995).
[9] D. Fussen and C. Kubach, J. Phys. B **19**, L31 (1986).
[10] J. Moseley, W. Aberth, and J. R. Peterson, Phys. Rev. Lett. **24**, 435 (1970).
[11] S. Szucs, M. Karemera, M. Terao, and F. Brouillard, J. Phys. B **17**, 1613 (1984).
[12] B. Peart and D. A. Hayton, J. Phys. B **25**, 5109 (1992).

[13] B. Peart, M. A. Bennett, and K. Dolder, J. Phys. B **18**, L439 (1985).
[14] B. Peart, S. J. Foster, and K. Dolder, J. Phys. B **22**, 1035 (1989).
[15] S. Geltman, *Topics in Atomic Collision Theory* (Krieger Publishing Co., Malabar, 1997).
[16] J. von Neumann and E. Wigner, Phys. Z. **30**, 467 (1929).
[17] D. R. Bates and R. McCarroll, Proc. R. Soc. London, Ser. A **245**, 175 (1958).
[18] J. B. Delos, Rev. Mod. Phys. **53**, 287 (1981).
[19] A. K. Belyaev, D. Egorova, J. Grosser, and T. Menzel, Phys. Rev. A **64**, 052701 (2001).
[20] D. W. Jepsen and J. O. Hirschfelder, J. Chem. Phys. **32**, 1323 (1960).
[21] C. A. Mead and D. G. Truhlar, J. Chem. Phys. **77**, 6090 (1982).
[22] M. Baer, Phys. Rep. **358**, 75 (2002).
[23] N. F. Mott and H. S. W. Massey, *The Theory of Atomic Colli-*

sions (Oxford University Press, London, 1965).

[24] M. Abramowitz and I. A. Stegun, *Handbook of Mathematical Functions* (Dover Publications, Inc., New York, 1972).

[25] B. R. Johnson, Phys. Rev. A **32**, 1241 (1985).

[26] M. L. Goldberger and K. M. Watson, *Collision Theory* (John Wiley & Sons, Inc., New York, 1964).

[27] B. R. Johnson, J. Comput. Phys. **13**, 445 (1973).

[28] D. E. Manolopoulos, M. J. Jamieson, and A. D. Pradhan, J. Comput. Phys. **105**, 169 (1993).

[29] F. Masnou-Seeuws and A. Salin, J. Phys. B **2**, 1274 (1969).

[30] L. Wolniewicz and K. Dressler, J. Chem. Phys. **88**, 3861 (1988).

[31] P. Quadrelli, K. Dressler, and L. Wolniewicz, J. Chem. Phys. **93**, 4958 (1990).

[32] L. Wolniewicz, J. Chem. Phys. **99**, 1851 (1993).

[33] L. Wolniewicz and K. Dressler, J. Chem. Phys. **100**, 444 (1994).

[34] L. Wolniewicz, J. Chem. Phys. **103**, 1792 (1995).

[35] L. Wolniewicz, J. Chem. Phys. **108**, 1499 (1998).

[36] G. Staszewska and L. Wolniewicz, J. Mol. Spectrosc. **212**, 208 (2002).

[37] T. Detmer, P. Schmelcher, and L. S. Cederbaum, J. Chem.

Phys. **109**, 9694 (1998).

[38] DALTON, a molecular electronic structure program, Release 2.0 (2005) (available online at http://www.kjemi.uio.no/software/dalton/dalton.html).

[39] T. H. Dunning, Jr., J. Chem. Phys. **90**, 1007 (1989).

[40] R. A. Kendall, T. H. Dunning, Jr., and R. J. Harrison, J. Chem. Phys. **96**, 6796 (1992).

[41] A. R. P. Rau, J. Astrophys. Astron. **17**, 113 (1996).

[42] V. Sidis, C. Kubach, and D. Fussen, Phys. Rev. A **27**, 2431 (1983).

[43] F. Borondo, A. Macias, and A. Riera, Chem. Phys. **81**, 303 (1983).

[44] A. S. Dickinson, R. Poteau, and F. X. Gadéa, J. Phys. B **32**, 5451 (1999).

[45] C. Galloy and J. C. Lorquet, J. Chem. Phys. **67**, 4672 (1977).

[46] A. J. Thakkar and T. Koga, Phys. Rev. A **50**, 854 (1994).

[47] F. Holka, P. Neogrády, V. Kellö, M. Urban, and G. H. F. Diercksen, Mol. Phys. **103**, 2747 (2005).

[48] W. Cheney and D. Kincaid, *Numerical Mathematics and Computing* (Brooks/Cole Publishing Co., Pacific Grove, 1985).

[49] X. Urbain (private communication).